CHARACTERIZATION OF SIMULATED MICROSTRUCTURES IN POLYDISPERSE PARTICLE DEPOSITION

Hern Kim[†] and Raj Rajagopalan*

Dept. of Chem. Eng., Myong Ji University, Yongin 449-728, Korea
*Dept. of Chem. Eng., Univ. of Houston, Houston, Texas 77204, U.S.A.

Abstract—The deposition of polydisperse particles under the influence of gravity is examined using computer simulation. A parameter, σ, that represents the standard deviation of particle size is used for studying the effect of the variation in polydispersity on the resulting microstructures. Structural correlations are examined through contact networks, radial and angular distribution functions, and diffraction patterns. The results show that the onset of ordering appears near $\sigma = 0.05$ as σ is decreased. The long-range ordering of the structures is not influenced by the introduction of a small amount of polydispersity, which may increase the uniformity of local density distribution in the angular direction. Polydisperse systems with small deviations in size display stronger positional order in some directions and this in turn contributes to the uniformity of overall packing structures.

INTRODUCTION

The packing problem has received considerable attention in chemical engineering [1] since the characteristics of packings (or, deposits, or sediments) influence transport phenomena in porous media, as in the case of fluid flow and heat transport in packed bed reactors and adsorption columns, filtration, drying of granular materials, diffusion and reaction in catalyst particles, etc. In the recent years the general class of packing problems further has relevance to deposition and coating phenomena and to the resulting microstructure of the deposits [2, 3]; for example, the fabrication of films and coatings via liquid-phase as well as vapor-phase deposition processes in fabrication of electronic, magnetic, and optical devices.

It is also important to note that most of the above studies have been mainly limited to monodisperse packings, although the use of polydisperse particles is more common in practice. One motivation for using polydisperse particulate systems is the existence of an optimum particle size distribution that maximizes the volume fraction of particles in a given packing. It is of very significant practical interest to determine such a particle size distribution. Another reason for the interest in polydisperse systems is the occurrence of a variety of packing problems such as mixing, percolation, segregation, etc., which are also practical sig-

nificance in many applications.

Studies of polydisperse systems have been confined mainly to binary mixtures of particles because of the resulting simplicity. Most of the useful information available for polydisperse systems is therefore restricted to binary mixtures regardless of whether the approach used is theoretical, experimental, or based on computer simulations; in particular, no systematic study of multicomponent systems with more than two components is available. In most cases, particle size distributions obtained in practice can be approximated with sufficient accuracy by continuous particle size distributions, which are determined in terms of just a few parameters. A few examples of previous studies which are relevant to the focus of the present paper and serve as background to this study are summarized in Table 1, where bulk properties such as packing fraction, porosity, and coordination number of the resulting structures as functions of particle characteristics and packing methods have been examined. In contrast, little information about the effects of particle size distribution on the variations in the structures of the deposits is available. Recently, interest has extended to (i) the effects of the local arrangement of particles on the overall packing structures, e.g., in the case of the sintering of ceramic powder compacts [9, 10], and (ii) the effect of polydispersity on phase behavior e.g., in the case of hard-sphere colloidal suspensions [11,12]. It is however surprising that, although the structures of the deposits frequently have aniso-

---

[†]To whom all correspondences should be addressed.

Table 1. A list of computer simulation approaches for random packing of polydisperse particles with a continuous size distribution

Authors	Type of polydispersity	Geometrical characteristics studied
Powell [4]	Log-normal	Packing fraction; Coordination number
Suzuki & Oshima [5]	Log-normal, Log-uniform Rosin-Rammler, Anderson	Void fraction; Coordination number
Rodriguez et al. [6]	Triangular	Packing fraction; Coordination number
Dickinson et al. [7]	Triangular	Packing fraction; Pore size distribution; Radial distribution function
Soppe [8]	Log-normal	Packing fraction; Pore size distribution; Radial distribution function; Coordination number

tropic properties, methods appropriate for characterizing the anisotropy have not been used in most cases.

The objectives of the present work are (i) to develop general characterization methods for analyzing microstructures of deposits and (ii) to investigate the effects of polydispersity on microstructure formation of deposits. The paper begins with a brief summary of the algorithm used and the essential computational details, which are available elsewhere [3]. Following this, the structural features of the packings (or, deposits) generated by the simulations are examined using local density distributions, diffraction patterns and so-called 'contact-network' diagrams.

DEPOSITION ALGORITHM

First a vertical strip into which the particles are deposited is considered. The particles, whose radii are already chosen from a given size distribution, enter this 'chamber' one by one from the top at random positions, distributed uniformly along the width of the chamber. Each particle falls along the direction of the external field (in this case, gravity) and comes into contact with either a previously deposited particle or the substrate. If the particle reaches and makes contact with the substrate, it is assumed to rest there permanently. If, on the other hand, it comes into contact with a previously deposited particles, it rolls down until it finds another particle or the substrate. If it makes contact with another particle, one determines if the current position of the rolling particle is stable. For this purpose, the position is assumed to be stable if the center of the rolling particle lies between the centers of two contacting particles. Otherwise, the rolling particle is allowed to continue to move (roll or fall, as the case may be), until a suitable host is found. This entire procedure is repeated until a predetermined number of particles is deposited. In order to

avoid boundary condition periodic boundary conditions are applied along the horizontal direction, where the periodicity of the strip is taken to be 40 times the particle diameter of unit length.

In the present work a particle size distribution is introduced in terms of Gaussian distribution given by

$$f(R) = \exp[-(R - R_{avg})^2/2\sigma^2]/(2\pi\sigma^2)^{1/2}, \qquad (1)$$

where R is the particle radius, R_{avg} is the average particle radius, and σ is the standard deviation in multiples of the average diameter of particle, which is also used here as a 'polydispersity index'. Fig. 1 shows the normal distribution of particle radii for different polydispersity indices. Also in order to keep the range of particle size reasonable, lower and upper cutoff limits are set at 0.1 and 0.9, respectively. Note that the cutoff limits do not affect the overall particle size distributions for σ smaller than 0.15 (see Fig. 1).

In the present work the individual effects of polydispersity on the structures of deposits are investigated. The results reported are based on the deposition of a total of 4,000 particles and the average over 25 configurations.

CHARACTERIZATION OF STRUCTURES

The structure of the deposits generated in the simulations is analyzed using contact-network diagram, diffraction patterns, and radial and angular distribution functions of particle positions. For calculating these, only those particles within ± 30% from the mid point are taken so that the influence of the substrate and of the free 'surface' at the top of the packing is avoided. The diffraction patterns are prepared using the structure factor S(q), which is defined by [13]

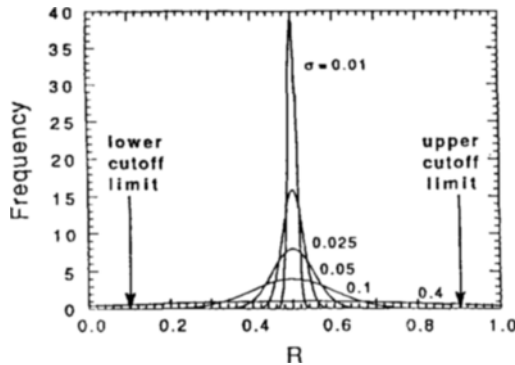$$S(\mathbf{q}) = (1/M) < |\Sigma \exp(i\mathbf{q} \cdot \mathbf{r}_j)|^2 >; \quad j = 1, \cdots, M \qquad (2)$$

Fig. 1. The normal distribution function of particle radii, $f(R) = \exp[-(R-R_{avg})^2/2\sigma^2]/(2\pi\sigma^2)^{1/2}$, where R_{avg} is the average radius and σ is the standard deviation.

where r_j is the position vector of the j-th particle, the summation is over all M particles in the chosen region, and the bracket $< \cdots >$ denotes the statistical average over the configurations.

The radial distribution function, $g(r)$, is a measure of the probability of finding two particles at any center-to-center separation r and is given by

$$g(r) = [\Delta n(r)/2\pi r\Delta r]/\rho_{avg} \qquad (3)$$

where $[\Delta n(r)/2\pi r\Delta r]$ is equal to $\rho(r)$, the local particle density, with $\Delta n(r)$ equal to the number of particles in the interval $[r, r+\Delta r]$. The function, $g(r)$, however, is suitable only for isotropic distributions of the particles. The above definition can be generalized to include the angular dependence of the density variation through

$$g(r, \theta) = [\Delta n(r, \theta)/r\Delta r\Delta\theta]/\rho_{avg} \qquad (4)$$

where $\Delta n(r, \theta)$ is the number of particles in the joint interval $[r, r+\Delta r]$ and $[\theta, \theta+\Delta\theta]$. In both Eqs. (3) and (4), ρ_{avg} is the overall average density of the packing.

The correlation length is defined using the variation of the function $\Psi(r)$ defined as

$$\Psi(r) = [(1/n)\Sigma\{g(r_i)-1\}^2]^{1/2}; \quad n=1,\cdots,M \qquad (5)$$

where $\{r_i, i=1,\cdots,M\}$ is the discrete set of r-values for which $g(r)$ has been calculated. In Eq. (5), r_1 corresponds to largest value of r for which $g(r)$ is available; r_1 is taken such that the value of $g(r_1)$ approaches the sufficiently asymptotic value of unity. The correlation length λ is then defined as
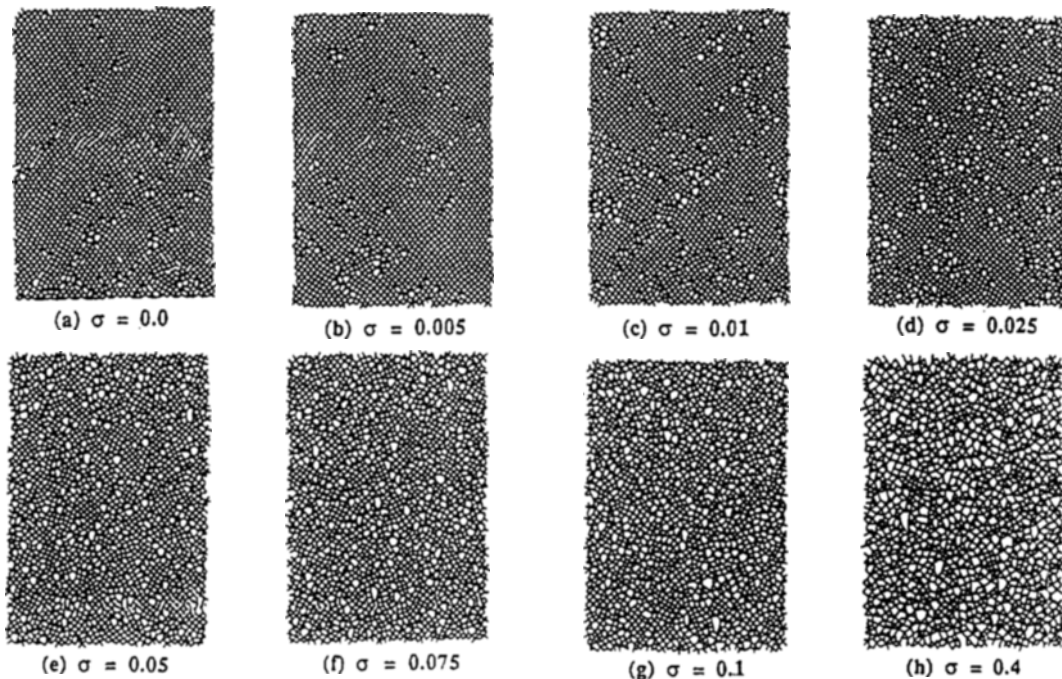

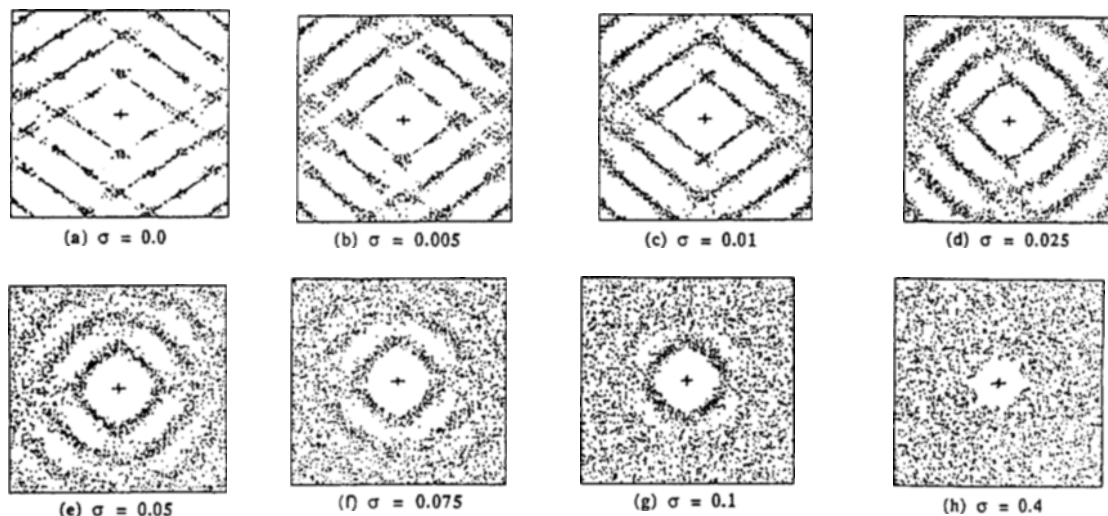Fig. 2. Contact networks corresponding to the packing structures.

(a) σ = 0.0   (b) σ = 0.005   (c) σ = 0.01   (d) σ = 0.025

(e) σ = 0.05   (f) σ = 0.075   (g) σ = 0.1   (h) σ = 0.4

Fig. 3. Diffraction patterns corresponding to the packing structures.

$$\lambda = r_n \quad \text{such that} \quad \Psi(r_n) = \varepsilon \qquad (6)$$

where ε is a small number < 1.

RESULTS AND DISCUSSIONS

First one can visually compare the structures that are generated as the polydispersity index is varied. Typical examples of the structures obtained for a set of selected values of σ are shown as the corresponding contact-network diagrams in Fig. 2. From this figure one notes a gradual change in the structure as the magnitude of σ is changed. It has been observed [2] that the particles tend to form ordered (crystalline) structures in the case of monodisperse packing (i.e., in the case of polydispersity index, σ, near zero). As the polydispersity index increases the ordering of the particles gradually disappears due to the gradual reduction in the uniformity of the particle sizes. A close look at Fig. 2 reveals that, as the polydispersity index increases, the number of polygons increases and their size becomes larger. It is also clear that the polygons are the source of defects. A large polygon in a contact network diagram may be due to a large pore surrounded by many particles or due to a collection of large particles. Small increases in σ lead to a frequent occurrence of defects such as stacking faults along ordered domains and tend to divide the ordered domains into smaller ones (see Figs. 2a-d for σ=0-0.0025). But as σ increases, polygonal defects appear randomly without any preferential direction, although small groups of rhombic units can still be found (see Figs. 2e-f for

σ=0.05-0.075). As the value of σ becomes larger, such ordered domains disappear completely and the basic unit in the structures changes from a rhombic cell to a mixture of polygons with small triangles (see Figs. 2g-h for σ=0.1-0.4).

Fig. 3 presents two-dimensional projections of the diffraction patterns for the structures shown in Fig. 2. It has been observed [2] that the diffraction pattern corresponding to σ=0 has two strong scattering directions. As the polydisperse index increases slightly, the scattering directions seem to remain unchanged, but the streaks along the two scattering directions become a little more diffuse (see Figs. 3b-c). As the polydispersity index becomes larger than 0.025, the scattering directions move away from each other and the diffraction patterns eventually become circular and diffuse, indicating the absence of sizable crystalline domains. This observation is very similar to that found in the packings of adhesive particles [2]. But such diffraction rings are observed only for σ near 0.025-0.05. Beyond this range of σ, the diffraction patterns tend to become diffuse significantly and the rings fade away rapidly at large q's. The first ring is still noticeable for σ as large as 0.1, but dissipates for larger σ's (see Fig. 3h, for σ=0.4).

The above observations are also illustrated in Fig. 4, which shows radial distribution functions, g(r), for a few values of σ. One can observe that the peaks for large r's disappear as σ increases, thus indicating the disappearance of the ordering in the structures. Note that the magnitude of g(r) in the near-field re-
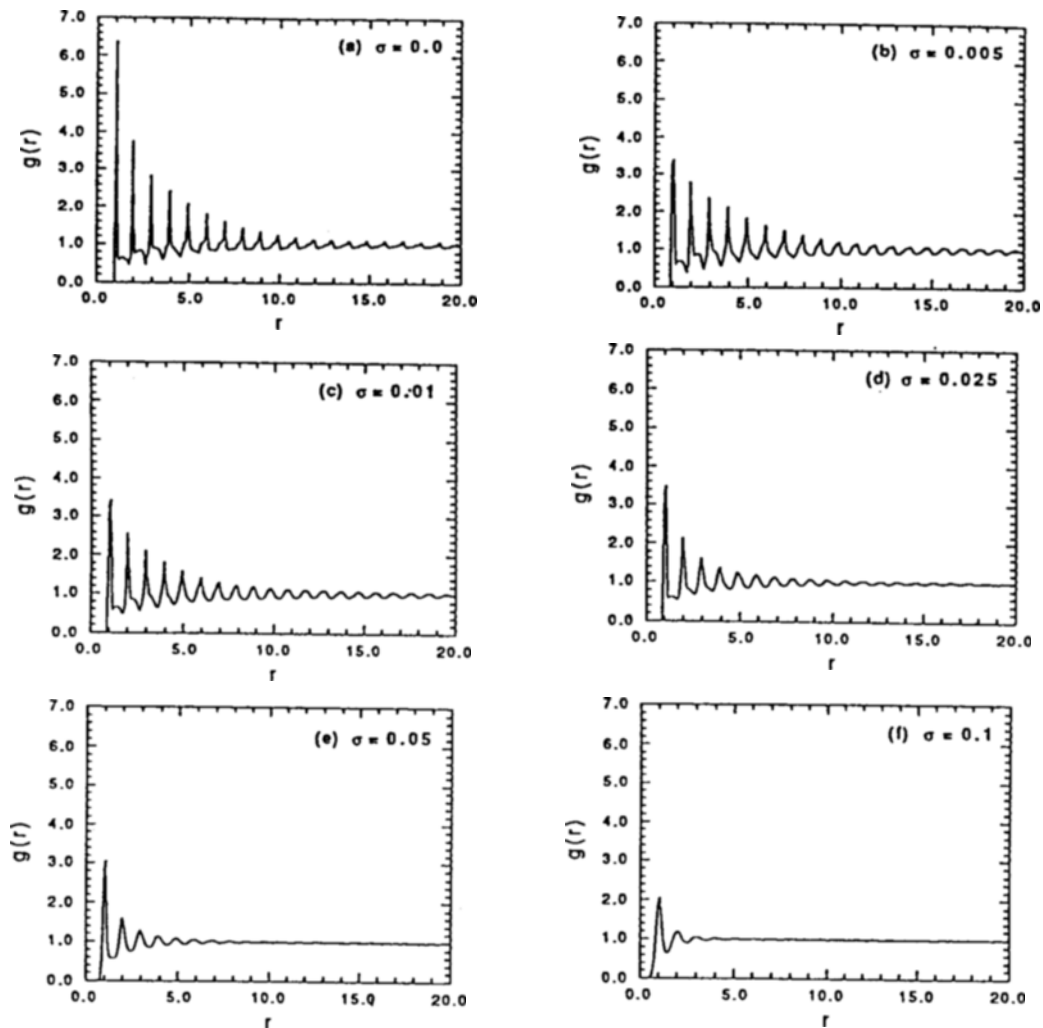
Fig. 4. The changes in the radial distribution functions, g(r), for different polydispersity indices.

gion is gradually reduced as σ increases, but the peaks still remain at large r's for smaller σ (see Figs. 4b-c). Also note that the peaks at large r for $\sigma=0$ are sharper than those when $\sigma=0.005$ or 0.01, but have more skewed shapes. Fig. 5 shows the correlation length obtained from the radial distribution function for different values of σ. Note a sharp decline in the correlation length with increasing σ for different λ indicating a sharp change from an ordered structure to a disordered one. Such a structural transition at a value of σ in the interval [0.025, 0.05] is consistent with the observation from the diffraction patterns shown in Fig. 3.
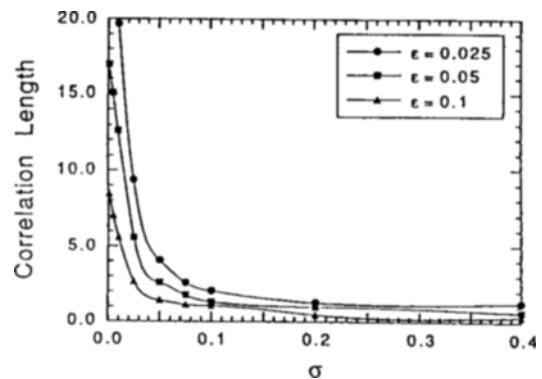
In addition, it is interesting to investigate the direc-

Fig. 5. Correlation lengths obtained from the radial distribution function, g(r), for different polydispersity indices.
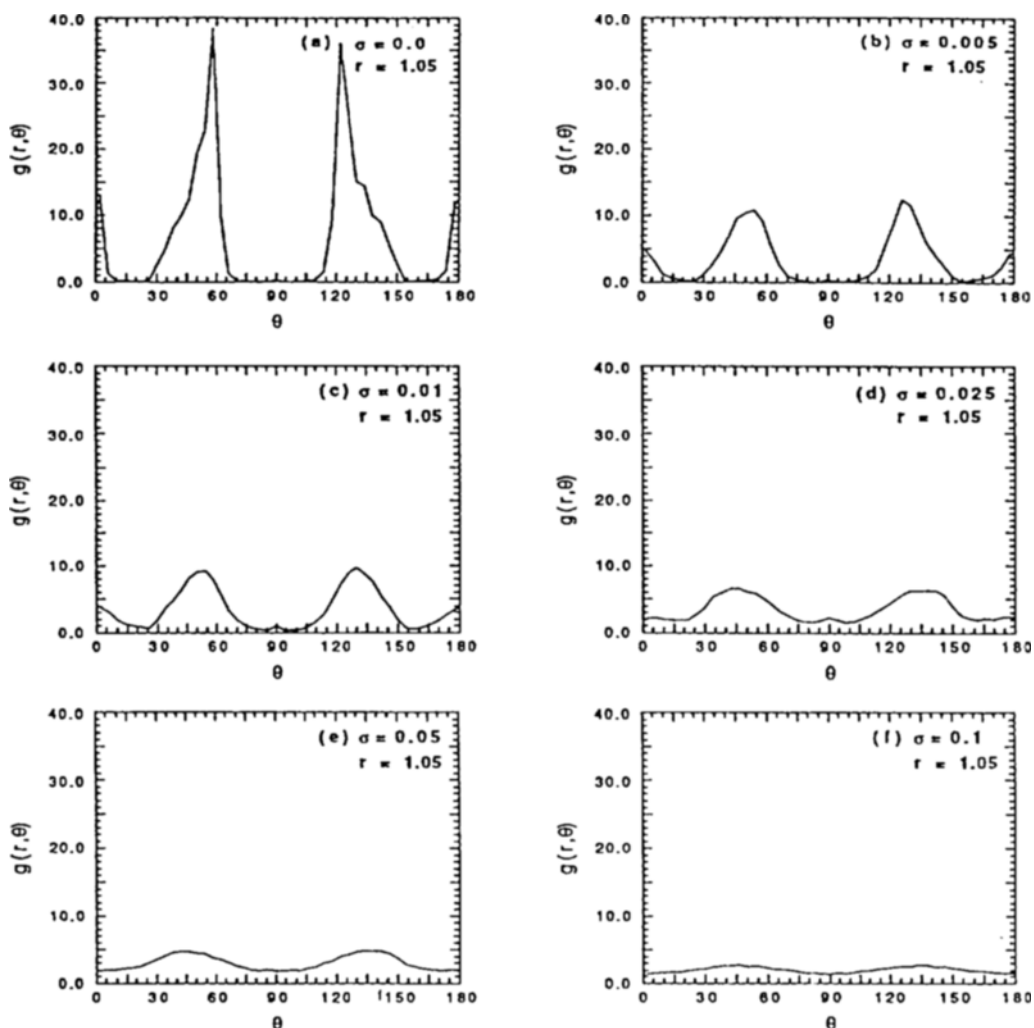
Fig. 6. Angular dependence of g(r, θ) at r = 1.05 for different polydispersity indices.

tional correlation in the packing structures as a function of σ. As illustrated in Fig. 6, from the near-neighbor value of g(r, θ) (i.e., for r = 1) for various σ, one observes two dominant angular directions along which there is a high probability of interparticle contact. With increases in σ, the sharp peaks shown from Fig. 6a for σ = 0 decrease rapidly and become broader, and the angle between the two peaks increases. But no other dominant direction of growth is found. The above observations are illustrated more quantitatively from normalized local density distributions, g(r, θ), along the radial and angular directions for a few values of σ. Consistent with the observations based on the diffraction patterns, one sees a monotonic decrease

in positional correlation for θ = 60° with increases in σ. But note that the long range of correlation is preserved along some directions (for θ = 45°). Note also that, while the peaks for σ = 0 show some disturbances, but those for nonzero but small σ's (i.e., σ = 0.005 and 0.01) become more stabilized and have higher values than those for σ = 0. Based on these, one can conclude that the introduction of a small amount of polydispersity (i.e., ~0.01) does not change the long-range ordering of the structures and may, in fact, increase the uniformity of local density distribution in the angular direction (also see Figs. 4a-c).

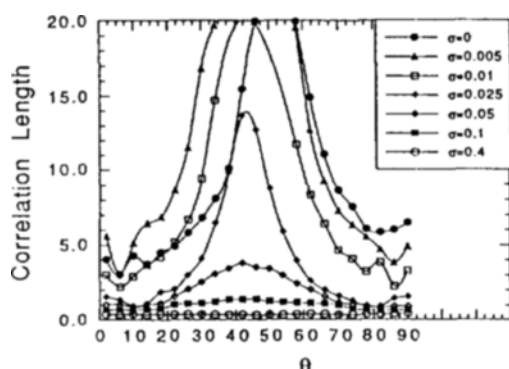The above observations can be clearly seen in the angular dependence of the correlation length on the

Fig. 7. Angular dependence of correlation lengths obtained from g(r, θ) for different polydispersity indices.

polydispersity index, shown in Fig. 7. This tendency is very similar to that observed at r=1.05 (see Fig. 6). Note that the correlation length has its maximum value within the range θ=30°-60°. The maximum tends to shift to the right (i.e., to higher angles). This indicates that packings with small polydispersity have a strong directionality with respect to long-range correlation. It is very interesting to investigate the variation of the correlation length with σ at each angle. For θ= ~50°-~90° and ~0°-~15° the correlation length decreases sharply as σ increases. This agrees well with the variation of the correlation length obtained from g(r) (see Fig. 6). But for θ= ~15°-~50° the correlation length shows a sharp increase with increasing σ for small values of σ (i.e., σ=0.005 and 0.01) and decreases sharply for large σ's. This observation becomes clearer when one examines g(r, θ) information for very small σ [2]. One can conclude from these that polydisperse systems with small deviations in size display stronger positional order in some directions and that this in turn contributes to the uniformity of overall packing structures. Also one can conclude that the onset of ordering (or crystallization) appears near σ=0.05 as σ is decreased (see Figs. 3, 5, and 7).

NOMENCLATURE

d   : diameter of the particle

g(r) : cylindrically averaged radial distribution function
g(r, θ) : positional correlation (distribution) function in r and θ
N   : total number of particles
q   : scattering vector
r   : position vector of a particle in real space
S(q) : static structure factor

Greek Letters

ε   : cutoff value of Ψ(r) defined in Eq. (6)
λ   : correlation length defined in Eq. (6)
θ   : angle between r and the horizontal direction
ρ(r) : local particle density
σ   : polydispersity index
Ψ(r) : function defining the correlation length

REFERENCES

1. Haughey, D. P. and Beveridge, G. S. G.: *Can. J. Chem. Eng.*, **47**, 130 (1969).
2. Kim, H. and Rajagopalan, R.: *Chem. Eng. Commun.*, **108**, 147 (1991).
3. Kim, H.: Ph. D. Dissertation, University of Houston, Houston, Texas, U.S.A. (1991).
4. Powell, M. J.: *Powder Technol.*, **25**, 45 (1980).
5. Suzuki, M. and Oshima, T.: *Powder Technol.*, **44**, 213 (1985).
6. Rodriguez, J., Allibert, C. H. and Chaix, J. M.: *Powder Technol.*, **47**, 25 (1986).
7. Dickinson, E., Milne, S. J. and Patel, M.: *Ind. Eng. Chem. Res.*, **27**, 1941 (1988).
8. Soppe, W.: *Powder Technol.*, **62**, 189 (1990).
9. Liniger, E. G. and Raj, R.: *J. Amer. Ceram. Soc.*, **71**, C408 (1988).
10. Madhavrao, L. and Rajagopalan, R.: *J. Mater. Res.*, **4**, 1251 (1989).
11. Lubetkin, S. D., Wedlock, D. J. and Edser, C. F.: *Colloids and Surfaces*, **44**, 139 (1990).
12. Davis, K. E., Russel, W. B. and Glantschnig, W. J.: *J. Chem. Soc. Farad. Trans.*, **87**, 411 (1991).
13. Hansen, J. P. and McDonald, I. R.: "Theory of Simple Liquids", 2nd ed., Academic Press, New York (1986).